ACS Energy LETTERS

http://pubs.acs.org/journal/aelccp

Conformably Skin-Adherent Piezoelectric Patch with Bioinspired Hierarchically Arrayed Microsuckers Enables Physical Energy Amplification

Da Wan Kim,[∞] Hyunseung Kim,[∞] Geon-Tae Hwang, Sung Beom Cho, Seung Hwan Jeon, Hyeon Woo Kim, Chang Kyu Jeong,* Sungwoo Chun,* and Changhyun Pang*

Cite This: *ACS Energy Lett.* 2022, 7, 1820–1827

Read Online

ACCESS | Metrics & More | Article Recommendations | Supporting Information

ABSTRACT: An intimate contact interface between wearable energy harvesting devices and nonflat human surfaces is critical for harvesting energy from the body's movements. The device can only absorb the deformation strain under stable interfacial adhesion to biological surfaces. Past developments have mainly examined the active layer of such devices, but the device/body adhesive interface effects are rarely considered. Here, we introduce a hierarchically arrayed octopus-inspired pattern (h-OP) formed on piezoelectric composite patch devices. The h-OP enables robust wet adhesion to skin because its dome-like architecture achieves interfacial adhesion by generating cohesive forces among liquid molecules. We used finite element method simulation to investigate decohesion behaviors with bending-induced stress distribution. The enhanced adhesion provided efficient energy generation under strain according to body movements. With 90° wrist bending, the h-OP devices demonstrated approximately triple the energy generation of implementations with no pattern, exhibiting stable adhesion and high energy generation efficiency, even on the wet skin.

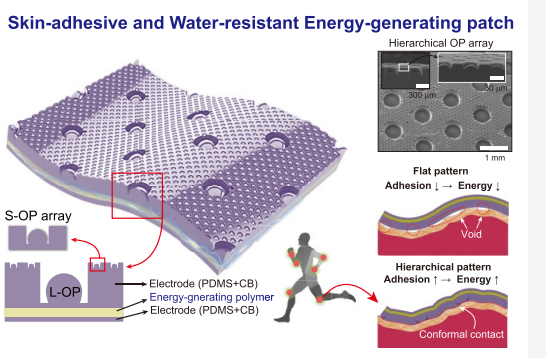

Wearable electronic devices that can be attached or worn over human surfaces have recently received considerable attention for application in the upcoming fields of intelligent technologies such as healthcare, robotics, energy, and biomedical applications.[1−3] However, such devices have short-term power supply problems, requiring complex power systems and regular charging. Recently, a method of applying self-powered energy harvesting technology to charge electronic devices has emerged as an alternative.[4−6] Technologies are being developed to construct a thin and lightweight self-powered wearable device by adapting piezoelectric and triboelectric principles, and they mostly generate energy through physical movements of the body, such as pulse, blood vessel flow, joint movement, and blinking.[7−9] Piezoelectric-based energy harvesting is a mainstream selection method because of its high power density, simple design, and high scalability under low strain changes.[10,11] For wearable applications, recent research has focused on lead-free piezoelectric materials that are biocompatible.[12,13] Despite of their high performance in wearable devices, there is one critical consideration for applying wearable electronic applications; that is, wearable energy harvesting devices exhibit low energy generation efficiency owing to low adhesion on biological skin.[14] As biological skin may be rough, wet, and mechanically soft, it is challenging to achieve conformal contact with the devices. When a stress is applied to generate energy from physical movements of the body, the devices slide on the skin surface owing to low interfacial adhesion, thus reducing the energy generation capability. Consequently, it is extremely advantageous to transform the movement-mediated kinetic energy into electrical potential to charge wearable electronic devices if the energy harvesting device is highly adhered to nonflat skin (often wet), although this is an extremely challenging process. However, there have been no studies

Received: February 3, 2022
Accepted: April 25, 2022
Published: April 28, 2022

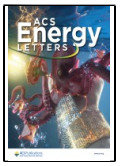

https://doi.org/10.1021/acsenergylett.2c00259
ACS Energy Lett. 2022, 7, 1820−1827

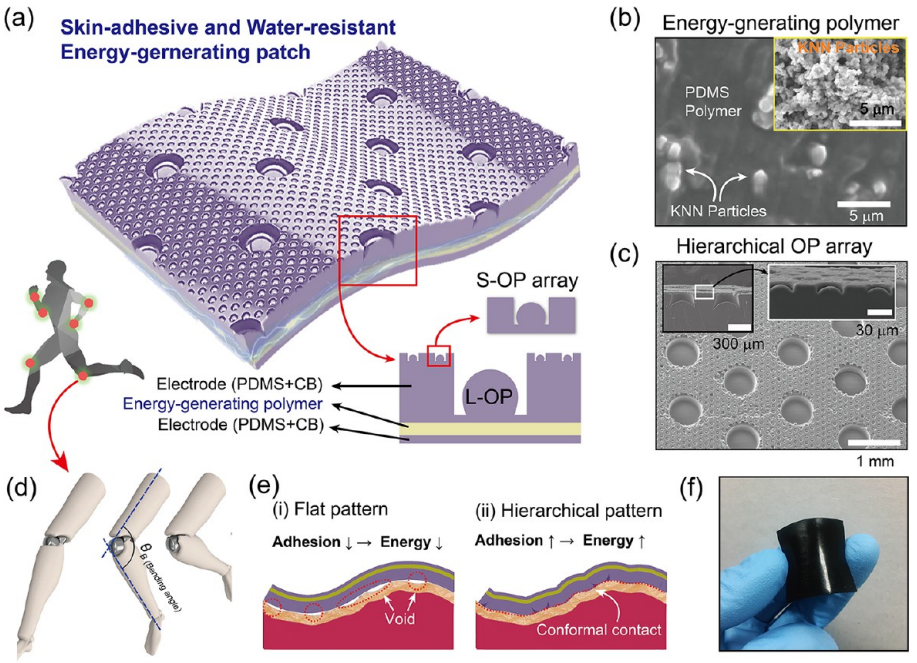

Figure 1. Reversible skin-adhesive energy-generating patch. (a) Schematic illustration of the hierarchical octopus-inspired patterns (h-OPs) array assembled with energy-generating polymer. (b) SEM image of the energy-generating polymer with PDMS and KNN particles. (c) SEM image of h-OPs array with protuberance-like dome-shaped structures (diameter: 30 and 300 μm). (d) Schematic of biomechanical hinges on the human body which can process bending deformation. (e) Schematic illustrations of cross-sectional profiles at interfaces of the patches and a rough skin surface (i) without and (ii) with the h-OPs. The harvested energy with h-OPs patch increases as the adhesion of h-OPs patch increases because of high skin-confomal property. (f) Image of the h-OP patch with high softness.

addressing adhesion to the skin to improve the efficiency of wearable energy-generating devices.

Chemical-based adhesives can be applied for achieving high adhesion to the skin. However, they may be not repetitive and may occasionally cause unwanted damages (e.g., flaking and redness) to the skin.[15,16] Thus, dry adhesives with high air permeability and repeatable use can prevent secondary skin damage, making them indispensable for realizing wearables and skin attachment devices. The recently developed convex structure (protuberance) of the suction chamber has shown remarkable adhesion performance even on dry, wet, and rough surfaces.[16−18] During the adhesion process, the capillary forces inside the suction chamber capture the residual water and create a complementary vacuum, which can improve the pulling strength of the adhesive for reusable, contamination-free, wet-resistive skin interface.

In this work, we report the efficacy of the robust adhesion of a wearable energy harvesting device to the skin, in increasing the energy generation efficiency. A hierarchically designed octopus-inspired pattern (h-OP) is used to amplify the energy generation efficiency because of the stable interfacial adhesion between the wearable piezoelectric composite patch and biological skin. On the basis of the finite element method simulation, we investigated decohesion behaviors with bending-induced stress distribution. The patch with the OPs shows approximately 3 times higher energy generation capability compared to the flat patch with bending of the wrist (90°). In addition, it has been proven that the OP's waterproof adhesion property allows OP to be used in wet environments.

We fabricated skin-adhesive wearable energy-harvesting patch devices by assembling stretchable polymer composite layers, as shown in Figure 1a and Figure S1. We first combined carbon black (CB)-based polymer composite electrodes on both sides of an energy-generating polymer composite with $K_{0.5}Na_{0.5}NbO_3$ (KNN) particle fillers (Figure 1b). The octopus-inspired h-OP was then formed on the skin-engaging surface of the energy-harvesting device (Figure 1c). The combination of hexagonal arrays of large octopus-inspired patterns (diameter of 300 μm, height of 300 μm, and spacing of 300 μm) and small octopus-inspired patterns (diameter of 30 μm, height of 30 μm, and spacing of 30 μm) maximizes the area of the suction chambers. Figure S2 shows the fabrication steps of the h-OP patch based on simple replica molding and microcontact printing techniques (see the Experimental Methods for details). The h-OP patch demonstrates excellent adhesion performance under dry or wet skin surfaces because the protuberance-like structure inside the chamber improves the suction stress owing to its structural properties.[16,17] As shown in Figure 1d, the joints of the human body can move at various bending angles. In particular, this movement of the human body requires high adhesion to rough and sweaty skin surfaces for efficient energy generation. Figure 1e shows a schematic illustration of the difference in energy generation capability owing to adhesion at the interfaces of the patches and a rough skin surface (i) without and (ii) with the h-OPs. The generated energy of patches with h-OPs increased with an increase in the adhesion of the h-OPs patch because of conformal contact with the skin surface. A good contact absorbs all the skin strain due to body movement and then induces a complete strain change in the device. Our self-energy-harvesting device with an h-OP patch with stretchable, conductive, and h-OP adhesive interface may be applied to wearable and skin-attached bioelectronics components (Figure 1f).

https://doi.org/10.1021/acsenergylett.2c00259
ACS Energy Lett. 2022, 7, 1820−1827

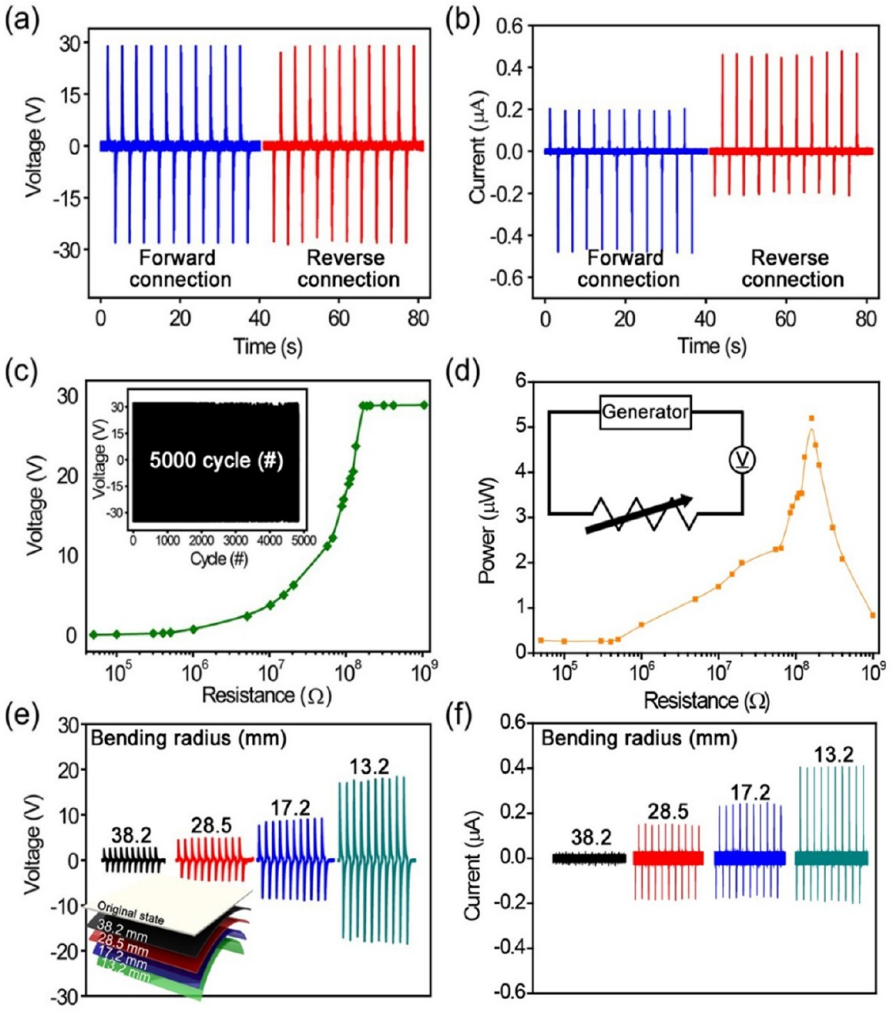

Figure 2. Measurement of the piezoelectric output signals from the KNN-PDMS energy harvesting devices under the bending and unbending motion. (a) Open-circuit voltage and (b) short-circuit current signals generated by the basic KNN-PDMS piezoelectric energy harvesting devices with flexible substrates in forward and reverse connections. (c) Generated measured voltage (V) according to the external circuit resistance (R). Inset: the durability of the energy-generating piezoelectric composite under ∼5000 repetitive operating conditions with stable energy harvesting performance. (d) Instantaneous power (P) as a function of the external load resistance calculated by $P = V^2/R$. (e) Piezoelectric voltage and (f) current signals generated by the composite energy harvesters with various bending angles.

To investigate the basic energy harvesting performance of our piezoelectric nanocomposite backbone, we fabricated a conventionally structured generator using an energy-generating piezoelectric composite composed of KNN particle fillers and a polydimethylsiloxane (PDMS) matrix with electrode-coated plastic substrates and an active layer (2.5 cm × 2.5 cm). KNN particles were well produced by a solid-state method, as shown by the X-ray diffraction pattern (Figure S3).[12] KNN was selected as the proper piezoelectric material because it is a highly biocompatible and high-performance lead-free piezoelectric ceramic.[19,20] Note that the mechanically neutral plane of a flexible piezoelectric device should be positioned asymmetrically in the thickness direction by the different thicknesses or mechanics of the top and bottom substrates in order to induce an effective strain in bending motion.[21,22] We used 40 wt % of KNN particles as the filler as they are high-performance piezoelectric composite generators.[21,23] For composite-type energy harvesters, d_{33} values have been used to evaluate piezoelectric properties.[24] The d_{33} piezoelectric coefficient of the manufactured piezoelectric composite film is 12.3 (±2.2) pC/N, which is similar to that of previous studies.[25,26] The piezoelectric signals were measured from the KNN-PDMS composite generator under bending and unbending motions in Figure 2. The uniform strain caused by external mechanical stress can generate a piezopotential in the piezoelectric composite. Figure 2a,b presents the open-circuit voltage and short-circuit current peaks generated by composite generator, respectively. The piezoelectric energy harvesting signal reaches up to ∼29 V and ∼0.2 μA when applying a bending motion (bending radius of ∼11.5 mm), respectively. The asymmetric shape of the current peaks is owing to the discrepancy in the bending and releasing motions of the customized bending machine because the current is related to the time scale. Additionally, the stress induces nonuniform piezoelectric potentials in the piezoelectric material inside the composite film, and an asymmetrical peak may occur due to the instantaneous current.[27] The composite generator connected with the measuring electrometer in the reverse connection shows the same levels for both voltage and current. This result proves that the recorded electrical signals are attributed to the piezoelectric effect of the KNN-PDMS composite generator.

https://doi.org/10.1021/acsenergylett.2c00259
ACS Energy Lett. 2022, 7, 1820−1827

Figure 2c shows that the measured voltage signals gradually increased with the external circuit resistance. The flexible KNN-PDMS composite device generated the highest voltage above the external load of 160 MΩ, similar to the open-circuit condition. In addition, a bending test (5000 cycles) was performed to measure the stability of the KNN-PDMS piezoelectric composite. In the inset of Figure 2c, the piezoelectric output was maintained by dropping the output value throughout the durability test. According to Ohm's law, the generated instantaneous power is calculated as a maximum value (approximately 5 μW) at ~160 MΩ, which indicates the matching impedance of the composite generator (Figure 2d).

Figure 2e,f shows the produced voltage and current signals under a variety of bending curvatures. The bending displacement was controlled using a customized bending equipment. When the bending radius of the flexible composite generator decreases and the bending strain becomes high, the piezoelectric energy harvesting signals also increase because of the increased piezoelectric potential. These curvature-dependent piezoelectric signals indicate that the KNN-PDMS piezoelectric composite can be robustly utilized for skin-attachable electronics, to harvest various biomechanical energies of our body hinges such as the elbow, wrist, and knee. For easier understanding, each bending radius of the flexible composite generator is converted into diverse body hinge angles, as illustrated in Figure 1d and Table S1.

Figure 3 shows the improvement of adhesion performances in dry and underwater conditions by the h-OPs. On the basis of the previous model, the h-OP of the domed structure is deformed by the applied preload, while at the same time the liquid molecules can be controlled to improve the wet adhesion.[17] The adhesion process of our h-OP model is described in Figure 3a−c. The deformed dome-shaped structure drains the residual liquid inside the s-OP chamber when the OP comes into contact with a wet surface by a low preload applied. After a larger preload is applied, the same phenomenon occurs with the L-OPs. When the external load is removed, elastic relaxation occurs the vacuum state in both the small and large chambers.[18,28] This is because the OPs create an enhanced suction effect by the capillary force on wet surfaces.[17,29] This result was confirmed by observing the drained water in the ring-shaped boundary of the OPs as shown in Figure 3b,c. When preload is applied, the water inside the chamber can be drained to the outside, and a vacuum is generated inside the chamber through the resulting empty space as shown in Figure S4. Figure 3d shows the performance of normal adhesion after applying various preloads to the silicon substrate in a dry environment. When considered as an axisymmetric detachment of an elastic film,[30] the dry adhesive stress ($\sigma_{o,dry}$) should take into account both the suction stress of the dry surface ($\sigma_{s,dry}$) and the van der Waals stress (σ_{vdw}): $(\sigma_{o,dry}) = (\sigma_{s,dry}) + (\sigma_{vdw})$.[31] At ambient conditions, the suction stress is created through the chamber volume change of the deformation behavior. In contrast, the van der Waals stress is determined by the engaged contact area of the substrate.[31] On the basis of the above equation, the theoretical adhesion forces were analyzed with the experimental measurements in various preloads (1−15 N/cm^2) under dry conditions. The normal adhesion (>7 N/cm^2) of the h-OP patch was 8 times higher than one (<2 N/cm^2) of a flat patch under dry conditions because of the suction stress effect.

The pulling-off adhesion force on the wafer substrate underwater conditions was measured, as shown in Figure 3e.

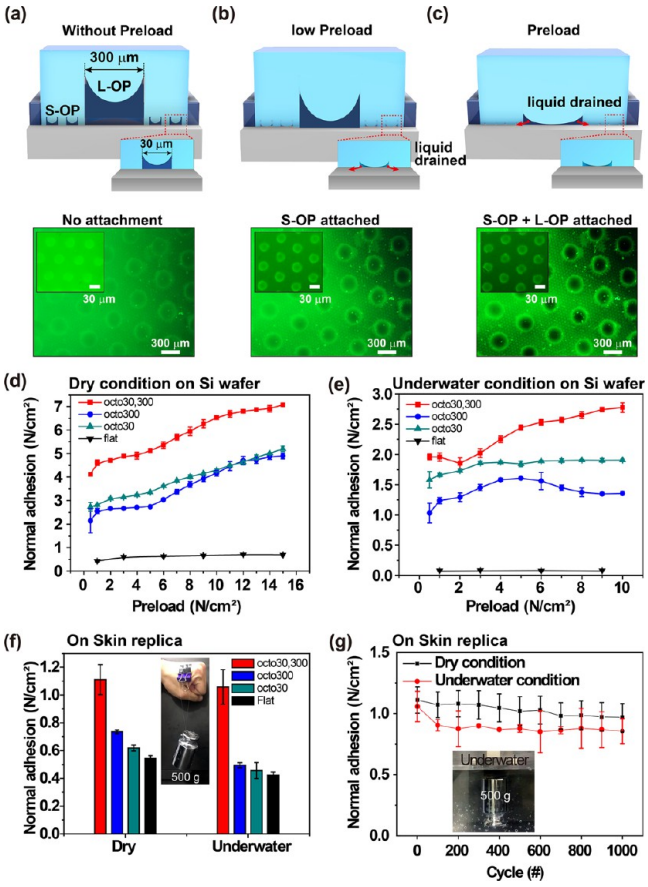

Figure 3. Measurement of pulling adhesion performance of a hierarchical OP film under various dry/wet conditions. (a−c) Schematic diagrams of the adhesion mechanism and the drained water at the OP boundary of the patch before (a) and after application of preloads of 2.0 N/cm^2 (b) and 10 N/cm^2 (c). (d, e) Comparison of measured vertical adhesion of samples with various preloads (1−15 N/cm^2) in dry (d) and underwater (e) environments against Si wafer substrates. (f) Pulling adhesion forces to OP patches and flat sample of skin replica after applying a preload of 2 N/cm^2. (g) Repeatability of the h-OP patches in dry and aquatic conditions on skin replicas. Error bars on the graph indicate standard deviation (N = 10).

In contrast to the adhesion on a dry surface, the suction ($\sigma_{s,wet}$) and capillary stresses ($\sigma_{c,wet}$) may be dominate under wet environments.[17] The underwater suction stress is expressed by the relationship among the material parameters of the adhesive patch $\left(\sqrt[3]{\frac{1-\nu^2}{E}}\right)$, geometric parameters of the L-OPs $\left(\frac{R_L k n_L \cdot (2R_L + l_L)}{\sqrt[3]{t_L r_{0,L}}}\right)$, S-OPs $\left(\frac{R_L k n_L \cdot (2R_S + l_S)}{\sqrt[3]{t_S r_{0,S}}}\right)$, and external preload $(F_p^{1/3})$.[17] The geometric parameters (radius of 15 μm for S-OPs and 150 μm for L-OPs) and material parameters (Poisson's ratio and Young's modulus of the sample) were considered, and the preload-dependent adhesion force is expressed as

https://doi.org/10.1021/acsenergylett.2c00259
ACS Energy Lett. 2022, 7, 1820−1827

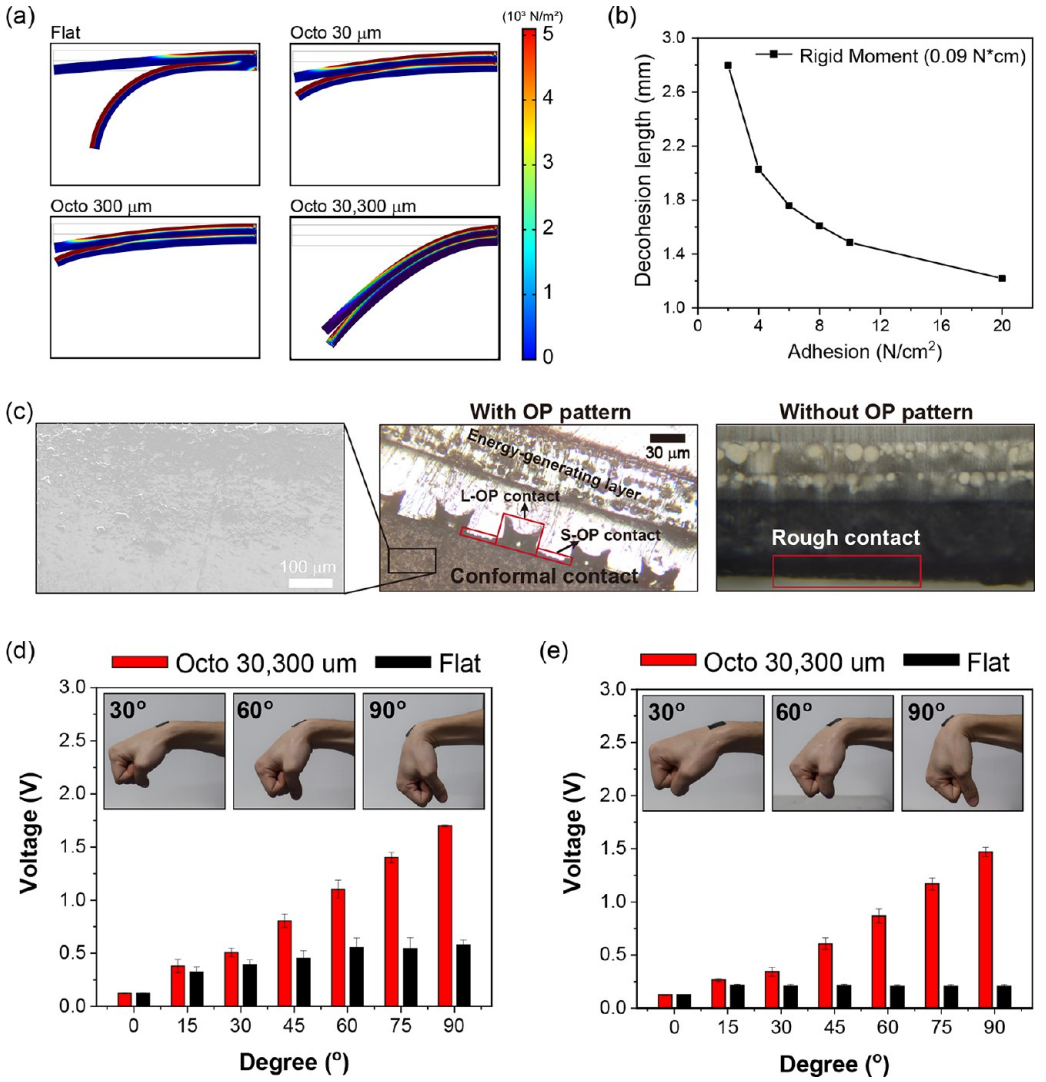

Figure 4. Application of the h-OP patch to energy harvesting on a human skin surface. (a) Finite element method simulation of various patch samples on a skin replica. (b) Adhesion strength versus a decohesion length at rigid moment (0.09 N·cm). (c) Cross-sectional SEM images at interfaces of the patches and skin replica without and with the h-OPs. Voids are not observed for the h-OP patch at the interface. The yellow dotted lines indicate voids due to incomplete contact by low adhesion force. Energy harvesting by the human movements with the hierarchical h-OP patch harvester in (d) dry and (e) wet conditions.

$$\sigma_{s,wet} \cong -2.145\left(\sqrt[3]{\frac{1-\nu^2}{E}}\right)\cdot kn_L R_L\left\{\frac{(2R_L + l_L)}{\sqrt[3]{t_L \cdot r_{0,L}}} + \frac{(2R_S + l_S)}{\sqrt[3]{t_S \cdot r_{0,S}}}\cdot\left(1 - \frac{\pi}{8\sqrt{3}}\right)\frac{R_L}{R_S}\right\}\Delta P \times F_p^{1/3} \quad (1)$$

where t is the depth of the OPs, ν is Poisson's ratio of the elastmer (PDMS, ~0.49), F_p is the preload, and r_0 is the radius of the dome in OPs. Since the adhesive is attached to a wet surface, its capillarity-mediated adhesion can be calculated using the Young−Laplace equation.[32] This includes both the water-resistant suction effect and the capillary-assisted stress of h-OP. In addition, the pulling adhesion of the h-OP patch was higher than that of a flat sample in wet conditions. To analyze the performance of the h-OP patch on the skin, we investigated the adhesion in the vertical direction to a porcine skin replica similar to human skin.[33] Figure 3f shows high pulling force (>1 N/cm^2) for the h-OP patch on the skin replica for dry/wet environments (see Figure S5). This contributes to the suction stress of h-OPs because liquids lose their van der Waals force-based adhesion.[34] As can be seen in Figure 3g, the h-OP patch retains its performance in reversible adhesion cycles (>1000) in both dry and underwater environments. These high reversible adhesion properties in wet environments have rarely been achieved with pillar dry adhesives.[35,36]

Figure 4 demonstrates the potential applications of the h-OP patch to self-powered energy harvesting patches combined with stretchable and conductive adhesive interfaces. In the case of human-attached energy devices, a large amount of energy can be produced by maintaining a steady angle without detachment from human motions. Therefore, on the basis of the simulation, we investigated the detachment process when bending deformation was applied to a human-attached patch. Figure 4a shows the bending-induced stress distribution and the visualized desorption of the human-attached device, depending on the type of patches and interface areas, but it highly depends on the decohesion behavior. The stress is concentrated at under the bending curvatures of the skin. The stress is mostly focused on the surface and the detached region

https://doi.org/10.1021/acsenergylett.2c00259
ACS Energy Lett. 2022, 7, 1820−1827

of the device, whereas the skin is more stressed in the attached region. The detachment area of the device is narrower with the octopus-patterned samples because they have higher adhesion than flat samples. However, at higher bending angles, it remained steady only in the case of hierarchical octopus patterns. This is because higher adhesion can reduce the decohesion behavior, as shown in Figure 4b. As a result, the higher the adhesion of the patch, the more piezoelectric energy can be harvested owing to the greater stress generated by the high bending deformation of the human body.

In the cross-sectional SEM image of the electronic patch attached to the pigskin replica, there are some voids at the interface between the flat patch and the skin replica due to lack of adhesion. However, the h-OP patch is in close contact with the skin replica without noticeable micro- and macropores due to the adhesive structures (Figure 4c). Figure 4d,e shows electrical energy harvesting by dynamic bending movements of the wrist in diverse environments using the flat patch and the h-OP patch. The bending tests were performed in distinguishable environments, as displayed in the inset images of Figure 4d,e.

The output voltage was gradually increased by increasing the bending angle from 0° to 90° in both dry and wet conditions. This is because the h-OP patches continually absorb the strain induced by bending deformation owing to the stable skin adhesion. Moreover, the h-OP patch can detect wrist bending even under wet conditions owing to its enhanced wet-tolerance. The bending-to-unbending operations (1000 cycles) were repeated to confirm reproducible energy generation ability on the wet wrist (Figure S6). However, the deformation applied to the wrist is not sufficiently applied to the patch under bending over 15° because the flat patch is detached from the skin surface. This is due to its high elasticity and repeatable adhesion performance to dry, wet, and rough skin, a result that is rarely achieved in recently studied self-energy harvesting electronics.

In summary, we developed a hierarchical skin patch with skin-attachable octopus-inspired patterns with water-resistance to obtain amplified energy output in wearable piezoelectric composite patches. With stable interfacial adhesion on the skin, the wearable patches can harvest electrical energy by efficiently transferring kinetic energy generated by human motion. We fabricated a conventionally structured generator using an energy-generating piezoelectric composite comprising KNN particle fillers and a polydimethylsiloxane (PDMS) matrix. The KNN-PDMS piezoelectric composite can be robustly utilized for wearable and skin-attachable energy or sensor devices. The piezoelectric composite patch with hierarchical OP provides high adhesion to dry and wet environments. We investigated the suction force of the hierarchical OPs by the geometric parameters (diameter of 30 μm for S-OPs and 300 μm for L-OPs) and material factors (Poisson's ratio and Young's modulus of the sample). Finally, we demonstrated the practical applications of the patches to skin-adhesive and water-resistant self-powered energy-harvesting devices. Our patch maintained high adhesion despite repeated detachment and showed energy production derived from joint movements of the human body without additional chemical adhesives. Although our KNN-based composite piezoelectric energy harvesting patch showed energy generation of 5 μW range, it is expected to be used as a self-generation source for small wireless electronic devices. In addition, it can be used not only as an energy source but also as a nonpowered sensor that is directly applied to the body as it is applied to a health care wearable device that is attached to the body or inserted into clothes to sense body movement.[37−40]

EXPERIMENTAL METHODS

Fabrication of KNN-PDMS Energy Harvesting Polymer Composite with OP Architectures. $K_{0.5}Na_{0.5}NbO_3$ (KNN) piezoelectric nanoparticles were synthesized using a solid-state reaction method. The mixed raw materials, i.e., K_2CO_3, Na_2CO_3, and Nb_2O_5 (purity >99%, Sigma-Aldrich) powder, were ball-milled overnight and calcined for 4 h at 850 °C to crystallize the perovskite structure. To obtain smaller-sized particles, the random-size KNN particles were remilled and crushed for 5 h. The average size of the KNN particles was approximately 300 nm. PDMS was used as the elastic matrix of the flexible piezoelectric nanocomposite. The prepolymer liquid and curing agent were blended at a ratio of 10:1 (w/w) to fabricate a polymer composite matrix solution. The KNN piezoelectric particles were added to the PDMS liquid and mixed for 3 h by magnetic stirring. The blended KNN-PDMS composite slurry was defoamed in a vacuum desiccator for 1 h to remove air bubbles. The piezoelectric nanocomposite slurry was spin-cast on a glass substrate and cured as a thick film at room temperature overnight. After curing, the poling process was applied to the piezoelectric composite film by an electric field of 1.2 kV for 3 h. The peeled-off flexible piezoelectric nanocomposite film was attached onto an indium tin oxide (ITO)-coated polyethylene terephthalate (PET) substrate or a carbon black-mixed PDMS conducting layer (CB-PDMS) as the bottom electrode to measure the basic piezoelectric signals of a conventional structured generator on a bending machine or the performance of OP-inspired skin-adhesive energy-generating patches on human skin, respectively. The piezoelectric coefficient (d_{33}) value was measured using a d_{33} meter (YE2730A, SINOCERA) at a fixed mechanical load condition of 110 Hz and 0.25 N. In order to optimize the size of the clamp, the flexible KNN-based composite film was set to the area of 1 × 1 cm^2. For the top electrode, another ITO-coated PET substrate or an octopus-inspired hierarchical architecture-arrayed CB-PDMS layer was used. The ITO-coated PET substrates were purchased from Sigma-Aldrich (100 nm thickness of the deposited ITO) with different thicknesses of PET (175 and 125 μm for bottom and top substrates, respectively). Note that the thicknesses of the bottom and top substrates should be different to localize the proper position of the mechanical neutral plane for the conventional structured generator with a device bending test for basic piezoelectric signals. Then, the OP architectures of the patch were stamped by microcontact printing (μ-CP) using a master of OPs and cured at 85 °C for 2 h on a Teflon substrate. Finally, the patches were obtained, as shown in Figure S2. The energy-harvesting patch was fabricated by connecting electrodes on top and bottom sides of the KNN-PDMS composite. The detailed method can be founded the Supporting Information.

ASSOCIATED CONTENT

Supporting Information

The Supporting Information is available free of charge at https://pubs.acs.org/doi/10.1021/acsenergylett.2c00259.

Experimental methods (piezoelectric measurements, normal adhesion measurements, simulation, and characterizations), detailed derivation of suction adhesion

https://doi.org/10.1021/acsenergylett.2c00259
ACS Energy Lett. 2022, 7, 1820−1827

and capillary adhesion (geometric and materials parameters), fabrication of the h-OP adhesive, X-ray diffraction (XRD), adhesion test environments, and the relationship of bending radius and bending angles (PDF)

AUTHOR INFORMATION

Corresponding Authors

Chang Kyu Jeong − *Division of Advanced Materials Engineering, Jeonbuk National University, Jeonju, Jeonbuk 54896, Republic of Korea; Department of Energy Storage/Conversion Engineering of Graduate School and Hydrogen and Fuel Cell Research Center, Jeonbuk National University, Jeonju, Jeonbuk 54896, Republic of Korea;* orcid.org/0000-0001-5843-7609; Email: ckyu@jbnu.ac.kr

Sungwoo Chun − *Department of Electronics and Information Engineering, Korea University, Sejong 30019, Republic of Korea*; Email: swchun127129@korea.ac.kr

Changhyun Pang − *Department of Chemical Engineering, Sungkyunkwan University, Suwon, Gyeonggi-do 16419, Republic of Korea; Samsung Advanced Institute for Health Sciences and Technology (SAIHST), Sungkyunkwan University, Suwon, Gyeonggi-do 16419, Republic of Korea;* orcid.org/0000-0001-8339-7880; Email: chpang@skku.edu

Authors

Da Wan Kim − *Department of Chemical Engineering, Sungkyunkwan University, Suwon, Gyeonggi-do 16419, Republic of Korea*

Hyunseung Kim − *Division of Advanced Materials Engineering, Jeonbuk National University, Jeonju, Jeonbuk 54896, Republic of Korea; Department of Energy Storage/Conversion Engineering of Graduate School and Hydrogen and Fuel Cell Research Center, Jeonbuk National University, Jeonju, Jeonbuk 54896, Republic of Korea*

Geon-Tae Hwang − *Department of Materials Science and Engineering, Pukyong National University, Busan 48513, Republic of Korea;* orcid.org/0000-0001-6151-3887

Sung Beom Cho − *Korea Institute of Ceramic Engineering and Technology (KICET), Jinju-si, Gyeonsangnam-do 52851, Republic of Korea;* orcid.org/0000-0002-3151-0113

Seung Hwan Jeon − *Department of Chemical Engineering, Sungkyunkwan University, Suwon, Gyeonggi-do 16419, Republic of Korea*

Hyeon Woo Kim − *Department of Virtual Engineering Center, Korea Institute of Ceramic Engineering and Technology (KICET), Jinju-si, Gyeonsangnam-do 52851, Republic of Korea; Division of Materials Science and Engineering, Hanyang University, Seoul 04763, Republic of Korea*

Complete contact information is available at: https://pubs.acs.org/10.1021/acsenergylett.2c00259

Author Contributions

[∞]D.W.K. and H.K. contributed equally to this work.

Notes

The authors declare no competing financial interest.

ACKNOWLEDGMENTS

We gratefully acknowledge the support from the National Research Foundation of Korea (NRF Grants 2019R1C1-C1008730, 2021R1F1A1059913, and 2022R1A2C4002037). This work was partially supported by a grant from Korea University.

REFERENCES

(1) Gong, S.; Cheng, W. Toward Soft Skin-like Wearable and Implantable Energy Devices. *Adv. Energy Mater.* **2017**, *7*, 1700648.

(2) Hua, Q.; Sun, J.; Liu, H.; Bao, R.; Yu, R.; Zhai, J.; Pan, C.; Wang, Z. L. Skin-inspired Highly Stretchable and Conformable Matrix Networks for Multifunctional Sensing. *Nat. Commun.* **2018**, *9*, 244.

(3) Pu, X.; Li, L.; Liu, M.; Jiang, C.; Du, C.; Zhao, Z.; Hu, W.; Wang, Z. L. Wearable Self-charging Power Textile Based on Flexible Yarn Supercapacitors and Fabric Nanogenerators. *Adv. Mater.* **2016**, *28*, 98−105.

(4) Guo, H.; Wen, Z.; Zi, Y.; Yeh, M. H.; Wang, J.; Zhu, L.; Hu, C.; Wang, Z. L. A Water-proof Triboelectric−electromagnetic Hybrid Generator for Energy Harvesting in Harsh Environments. *Adv. Energy Mater.* **2016**, *6*, 1501593.

(5) Pu, X.; Liu, M.; Chen, X.; Sun, J.; Du, C.; Zhang, Y.; Zhai, J.; Hu, W.; Wang, Z. L. Ultrastretchable, Transparent Triboelectric Nanogenerator as Electronic Skin for Biomechanical Energy Harvesting and Tactile Sensing. *Sci. Adv.* **2017**, *3*, No. e1700015.

(6) Siddiqui, S.; Kim, D.-I.; Duy, L. T.; Nguyen, M. T.; Muhammad, S.; Yoon, W.-S.; Lee, N.-E. High-Performance Flexible Lead-free Nanocomposite Piezoelectric Nanogenerator for Biomechanical Energy Harvesting and Storage. *Nano Energy* **2015**, *15*, 177−185.

(7) Fuh, Y.-K.; Chen, P.-C.; Huang, Z.-M.; Ho, H.-C. Self-powered Sensing Elements Based on Direct-write, Highly Flexible Piezoelectric Polymeric Nano/microfibers. *Nano Energy* **2015**, *11*, 671−677.

(8) Shi, B.; Li, Z.; Fan, Y. Implantable Energy-harvesting Devices. *Adv. Mater.* **2018**, *30*, 1801511.

(9) Wu, N.; Cheng, X.; Zhong, Q.; Zhong, J.; Li, W.; Wang, B.; Hu, B.; Zhou, J. Cellular Polypropylene Piezoelectret for Human Body Energy Harvesting and Health Monitoring. *Adv. Funct. Mater.* **2015**, *25*, 4788−4794.

(10) Bowen, C.; Kim, H.; Weaver, P.; Dunn, S. Piezoelectric and Ferroelectric Materials and Structures for Energy Harvesting Applications. *Energy Environ. Sci.* **2014**, *7*, 25−44.

(11) Li, H.; Tian, C.; Deng, Z. D. Energy Harvesting from Low Frequency Applications Using Piezoelectric Materials. *Applied physics reviews* **2014**, *1*, 041301.

(12) Peddigari, M.; Palneedi, H.; Hwang, G.-T.; Lim, K. W.; Kim, G.-Y.; Jeong, D.-Y.; Ryu, J. Energy Harvesting from Low Frequency Applications Using Piezoelectric Materials. *ACS Appl. Mater. Interfaces* **2018**, *10*, 20720−20727.

(13) Xu, S.; Hansen, B. J.; Wang, Z. L. Piezoelectric-Nanowire-Enabled Power Source for Driving Wireless Microelectronics. *Nat. Commun.* **2010**, *1*, 93.

(14) Lee, Y.; Park, J.; Choe, A.; Cho, S.; Kim, J.; Ko, H. Mimicking Human and Biological Skins for Multifunctional Skin Electronics. *Adv. Funct. Mater.* **2020**, *30*, 1904523.

(15) Laulicht, B.; Langer, R.; Karp, J. M. Quick-release Medical Tape. *Proc. Natl. Acad. Sci. U. S. A.* **2012**, *109*, 18803−18808.

(16) Chun, S.; Kim, D. W.; Baik, S.; Lee, H. J.; Lee, J. H.; Bhang, S. H.; Pang, C. Conductive and Stretchable Adhesive Electronics with Miniaturized Octopus-like Suckers against Dry/wet Skin for Biosignal Monitoring. *Adv. Funct. Mater.* **2018**, *28*, 1805224.

(17) Baik, S.; Kim, D. W.; Park, Y.; Lee, T.-J.; Bhang, S. H.; Pang, C. A Wet-tolerant Adhesive Patch Inspired by Protuberances in Suction Cups of Octopi. *Nature* **2017**, *546*, 396−400.

(18) Tramacere, F.; Pugno, N. M.; Kuba, M. J.; Mazzolai, B. Unveiling the Morphology of the Acetabulum in Octopus Suckers and Its Role in Attachment. *Interface focus* **2015**, *5*, 20140050.

(19) Park, S.; Peddigari, M.; Kim, J. H.; Kim, E.; Hwang, G.-T.; Kim, J.-W.; Ahn, C.-W.; Choi, J.-J.; Hahn, B.-D.; Choi, J.-H.; et al. Selective

Phase Control of Dopant-free Potassium Sodium Niobate Perovskites in Solution. *Inorg. Chem.* **2020**, *59*, 3042−3052.
(20) Zhang, Y.; Kim, H.; Wang, Q.; Jo, W.; Kingon, A. I.; Kim, S.-H.; Jeong, C. K. Progress in Lead-free Piezoelectric Nanofiller Materials and Related Composite Nanogenerator Devices. *Nanoscale Advances* **2020**, *2*, 3131−3149.
(21) Kim, H.; Sohn, C.; Hwang, G.-T.; Park, K.-I.; Jeong, C. K. $(K,Na)NbO_3$-$LiNbO_3$ Nanocube-based Flexible and Lead-free Piezoelectric Nanocomposite Energy Harvesters. *J. Korean Ceram. Soc.* **2020**, *57*, 401−408.
(22) Lee, G.-J.; Lee, M.-K.; Park, J.-J.; Hyeon, D. Y.; Jeong, C. K.; Park, K.-I. Piezoelectric Energy Harvesting from Two-dimensional Boron Nitride Nanoflakes. *ACS Appl. Mater. Interfaces* **2019**, *11*, 37920−37926.
(23) Lee, K. Y.; Kim, D.; Lee, J. H.; Kim, T. Y.; Gupta, M. K.; Kim, S. W. Unidirectional High-Power Generation via Stress-Induced Dipole Alignment from ZnSnO3 Nanocubes/Polymer Hybrid Piezoelectric Nanogenerator. *Adv. Funct. Mater.* **2014**, *24*, 37−43.
(24) Kim, Y.; Kim, H.; Lee, G.-J.; Lee, H.-U.; Lee, S. G.; Baek, C.; Lee, M.-K.; Park, J.-J.; Wang, Q.; Cho, S. B.; Jeong, C. K.; Park, K.-I. Flexoelectric-boosted Piezoelectricity of $BaTiO_3$@$SrTiO_3$ Core-shell Nanostructure Determined by Multiscale Simulations for Flexible Energy Harvesters. *Nano Energy* **2021**, *89*, 106469.
(25) Deutz, D. B.; Mascarenhas, N. T.; van der Zwaag, S.; Groen, W. A. Enhancing Energy Harvesting Potential of $(K,Na,Li)NbO_3$-Epoxy Composites via Li Substitution. *J. Am. Ceram. Soc.* **2017**, *100*, 1108−1117.
(26) Deutz, D. B.; Mascarenhas, N. T.; van der Zwaag, S.; Groen, W. A. Poling Piezoelectric $(K,Na,Li)NbO_3$-polydimethylsiloxane Composites. *Ferroelectrics* **2017**, *515*, 68−74.
(27) Jeong, C. K.; Park, K.-I.; Ryu, J.; Hwang, G.-T.; Lee, K. J. Large-Area and Flexible Lead-Free Nanocomposite Generator Using Alkaline Niobate Particles and Metal Nanorod Filler. *Adv. Funct. Mater.* **2014**, *24*, 2620−2629.
(28) Tramacere, F.; Beccai, L.; Kuba, M.; Gozzi, A.; Bifone, A.; Mazzolai, B. The Morphology and Adhesion Mechanism of Octopus Vulgaris Suckers. *PLoS One* **2013**, *8*, No. e65074.
(29) Su, Y.; Ji, B.; Huang, Y.; Hwang, K. Effects of Contact Shape on Biological Wet Adhesion. *J. Mater. Sci.* **2007**, *42*, 8885−8893.
(30) Afferrante, L.; Carbone, G.; Demelio, G.; Pugno, N. Adhesion of Elastic Thin Films: Double Peeling of Tapes Versus Axisymmetric Peeling of Membranes. *Tribol. Lett.* **2013**, *52*, 439−447.
(31) Heepe, L.; Varenberg, M.; Itovich, Y.; Gorb, S. N. Suction Component in Adhesion of Mushroom-shaped Microstructure. *J. R. Soc., Interface* **2011**, *8*, 585−589.
(32) Bullock, J. M. R. *Biomechanics of the Fibrillar Adhesive System in Insects*; University of Cambridge, 2010.
(33) Yang, S. Y.; O'Cearbhaill, E. D.; Sisk, G. C.; Park, K. M.; Cho, W. K.; Villiger, M.; Bouma, B. E.; Pomahac, B.; Karp, J. M. A Bio-inspired Swellable Microneedle Adhesive for Mechanical Interlocking with Tissue. *Nat. Commun.* **2013**, *4*, 1702.
(34) Huber, G.; Mantz, H.; Spolenak, R.; Mecke, K.; Jacobs, K.; Gorb, S. N.; Arzt, E. Evidence for Capillarity Contributions to Gecko Adhesion from Single Spatula Nanomechanical Measurements. *Proc. Natl. Acad. Sci. U. S. A.* **2005**, *102*, 16293−16296.
(35) Kwak, M. K.; Jeong, H. E.; Suh, K. Y. Rational Design and Enhanced Biocompatibility of a Dry Adhesive Medical Skin Patch. *Adv. Mater.* **2011**, *23*, 3949−3953.
(36) Drotlef, D. M.; Amjadi, M.; Yunusa, M.; Sitti, M. Bioinspired Composite Microfibers for Skin Adhesion and Signal Amplification of Wearable Sensors. *Advanced materials* **2017**, *29*, 1701353.
(37) Ham, S. S.; Lee, G.-J.; Hyeon, D. Y.; Kim, Y.; Lim, Y.; Lee, M.-K.; Park, J.-J.; Hwang, G.-T.; Yi, S.; Jeong, C. K.; Park, K.-I. Kinetic Motion Sensors Based on Flexible and Lead-free Hybrid Piezoelectric Composite Energy Harvesters with Nanowires-embedded Electrodes for Detecting Articular Movements. *Composites Part B: Engineering* **2021**, *212*, 108705.
(38) Shi, K.; Sun, B.; Huang, X.; Jiang, P. k. Synergistic Effect of Graphene Nanosheet and $BaTiO_3$ Nanoparticles on Performance Enhancement of Electrospun PVDF Nanofiber Mat for Flexible Piezoelectric Nanogenerators. *Nano Energy* **2018**, *52*, 153−162.
(39) Yaqoob, U.; Uddin, A.S.M. I.; Chung, G.-S. A Novel Tri-layer Flexible Piezoelectric Nanogenerator Based on Surface-modified Graphene and PVDF-$BaTiO_3$ Nanocomposites. *Appl. Surf. Sci.* **2017**, *405*, 420−426.
(40) Siddiqui, S.; Kim, D.-I.; Roh, E.; Duy, L. T.; Trung, T. Q.; Nguyen, M. T.; Lee, N.-E. A Durable and Stable Piezoelectric Nanogenerator with Nanocomposite Nanofibers Embedded in an Elastomer under High Loading for a Self-powered Sensor System. *Nano Energy* **2016**, *30*, 434−442.

NOTE ADDED AFTER ASAP PUBLICATION

Published ASAP on April 28, 2022; Revised May 5, 2022 to correct production error in Figure 2.

https://doi.org/10.1021/acsenergylett.2c00259
ACS Energy Lett. 2022, 7, 1820−1827